ATMOSPHERIC SMOG MODELLING, USING EOS SATELLITE ASTER IMAGE SENSOR, WITH FEATURE EXTRACTION FOR PATTERN RECOGNITION TECHNIQUES AND ITS ANALYSIS OF VARIANCE WITH IN-SITU GROUND SENSOR DATA

Parthasarathi Roy[1*], Paul Beaty[1**], J. O. Brumfield[2], Ralph Oberly[2], Anita Walz [3] , John Pollard[1], Jeff Dooley[1], Paul Kennedy[1] and Jeff Dooley[1]

[1]ERDAS, Inc., 5051, Peachtree Corners Circle, Norcross, Georgia, 30092 -(Parthasarathi.Roy, Paul.Beaty, John.Pollard, Paul.Kennedy. Jeff.Dooley@erdas.com)
[2]Graduate Program in Physical Sciences, Marshall University (oberly, brumfiel@marshall.edu)
[3]Department of Geography, Marshall University (walz@marshall.edu) One John Marshall Drive, Huntington, WV 25755

KEY WORDS: Smog, Absorption Bands, Satellite-Imagery, Spectral Signature, Sensors, and ASTER.

ABSTRACT:

Atmospheric pollution was previously considered as a 'Brown Cloud' phenomenon restricted to industrialized urban regions. Studies in field stations and satellite observations made since the last decade revealed that it now spans continents and ocean basins world wide. Anthropogenic activities are considered to be the primary cause of pollution in the atmosphere. The appearance of a smog layer with more absorption and scattering of solar radiations, particularly long-wave infrared radiations, decreases the atmospheric transmission factor, significantly perturbing the atmospheric absorption of solar radiation. The objective of this research is to create a geo-spatial model based on probability density of common atmospheric pollutants in the troposphere by using feature extraction and pattern recognition technique with high-spectral and spatial resolution Earth Observation System (EOS) satellite imaging sensor Advanced Spaceborne Thermal Emission and Reflection Radiometer (ASTER) data, US Environmental Protection Agency (EPA) ground sensor data and "Analysis of Variance" of satellite pixel value with EPA ground sensor observations. This research investigated three locations: 1. San Francisco Bay area, in California has a unique land feature having maritime climate surrounded by coastal ranges. 2. Los Angeles, in California (a maritime climate) and, 3. Charleston, in West Virginia which has humid continental climate in the mountain ranges in Kanawha Valley. Polluting industries data and Tapered Element Oscillating Microbalance (TEOM) ground sensor data are collected from the US-EPA. Spectral signatures of common atmospheric pollutants are collected from Jet Propulsion Laboratory's ASTER spectral Library, HITRAN Database, and USGS spectral library. Climatic data are collected from National Oceanic and Atmospheric Administration - National Climatic Data Center (NOAA-NCDC). All spatial data are stored as point features in shapefiles, with pollutants concentration as attributes in ArcGIS 9.2 software and imported into ER Mapper vector files for locating ground sensors and pollutants sources in ASTER imagery. ASTER L1B data are georegistered and geocorrected by image-to-image registration with georegistered Digital Orthophoto Quarter-Quadrangles (DOQQ's). Principal Component Analysis, Density Slicing and Band Ratioing techniques are applied to extract features in the ASTER datasets. Spectral signatures in graphical form of the atmospheric features are obtained in ER-Mapper 7.1 geospatial software and compared both in short wave infra-red (SWIR) and thermal infra-red (TIR) bands. Correlation between ground sensor pollution level and ASTER image pixel digital numbers are investigated in the study of Analysis of Variance, by creating a general linear model in SAS software It is observed that there is significant city effect, suggesting different kinds of atmospheric pollutants in different cities under investigation. Despite the broader bandwidth of ASTER as compared to hyperspectral satellite systems, it is observed that TIR band 14 is highly correlated with EPA monitored concentration in NOx and PM_{10} and SWIR band 7 is moderately correlated with EPA monitored CO concentration data in all the three areas, (i.e. San Francisco Bay area and Los Angeles, in California, and in Charleston in West Virginia). Future investigation is envisioned to study the subtle differences in spectral signatures of air pollutants by using hyperspectral satellite data and advanced sensors.

1. INTRODUCTION

Although atmospheric pollution was previously considered as a 'Brown Cloud' phenomenon restricted to industrialized urban regions, studies in field stations and satellite observations made since the last decade revealed that it now spans continents and ocean basins worldwide (RETALIS, 1999). Anthropogenic activities are considered to be the primary cause of pollution in the atmosphere. Secondary pollutants are created from the primary pollutants by complex photochemical reactions in the presence of ultra-violate (UV) radiation forming free radicals in the atmosphere (UNEP 2005). Gaseous air pollutants, like NO_x, SO_2 , CO, and CH_4 , are some of the primary air pollutants in urban and industrial areas. In the presence of atmospheric moisture, NO_x transforms into HNO_3 and HNO_2 (WHO, 2000). Air pollutants can be found in all three physical phases: solid, liquid or gaseous. When pollutants are in fine solid state floated in the atmosphere, they are called aerosols or particles, which depending on their diameter, can be non-respirable particles (of dimension greater than 10 μ m), respirable particulate matter, PM_{10} (of dimension less than 10 μ m), or inhalable particulate matter, $PM_{2.5}$ (of dimension less than 2.5 μ m). Both PM_{10} and $PM_{2.5}$ can remain in suspension in the air for hours or days and can be transported by the wind to significant distances.

1.1 Radiative Forcing:

Smog affects the earth's energy budget directly by scattering and absorbing radiation and indirectly by acting as cloud condensation nuclei and, thereby, affecting cloud properties (Yu, 2005). The appearance of a pollution layer with more absorption and scattering of solar radiations, particularly long-wave infrared radiations, decreases the atmospheric transmission factor, and changes the radiation fluxes, not only at the ground surface, but also at the top of the atmosphere, thereby significantly perturbing the atmospheric absorption of solar radiation (Ramanathan and Ramanna, 2003). These aerosol-induced changes in the radiation budget are referred to as 'radiative forcing' Furthermore, the pollution layer in atmosphere absorbs as well as emits radiance thus causing a change of the upwelling radiation.

1.2 Spectral Signature of Common Atmospheric Pollutants

IR absorption spectroscopy has played an important role in the identification of trace pollutants in both ambient air and synthetic smog systems. In absorption spectroscopy, solar radiation transfers its energy to molecules. Molecular vibration and rotation occur when the frequency of rotation and vibration are equal to frequency of solar radiation directed to the molecules. The molecule absorbs the radiation energy. Spectral signatures of common atmospheric pollutants are collected from Jet Propulsion Laboratory (JPL)'s ASTER (Advanced Spaceborne Thermal Emission and Reflection Radiometer) spectral Library, HITRAN (High-resolution Transmission Molecular Absorption) Database (HITRAN database), and USGS (United States Geological Survey) spectral library (USGS, 1998). Some of the common air pollutants spectral absorption frequencies along with associated ASTER bands are shown in table1 below.

Air Pollutants	Absorption Frequency in μ m	ASTER corresponding Band
Carbon Monoxide	2.30-2.34	7,8,9
HNO3	11	14
CH3OH	8.1	10
Hydroxyl Radical	2.1, 2.3-2.34	5,7,9
Zn,Fe-Sulfide	2.3	7
Arsenite	2.1-2.5	5,6,7,8,9
Formaldehyde	5.3	No Bands
SO2	8.1	9,10,11
Cirrus Cloud	2.1	5
Water Vapor	1.67	4
CaCO3	5.3-12.0	10,11,12,13,14
Particulate Matters	6.0 - 13.0	10,11,12,13,14
Methane	4.6	No bands

Table1: Spectral Signatures (absorption frequencies of common air pollutant, and corresponding ASTER bands (Sources: JPL. USGS, HITRAN, Herzberg, 1950).

1.3 Satellite Remote Sensing

Satellite image data consists of earth radiances observed by its sensors in different bands. For thermal infra-red (TIR) bands the radiances represent a function of the temperature, emissivity of the ground surface and the atmospheric column above and it's surrounding (ASTER, 2000). Satellite data can be used quantitatively to validate air quality models. It is now possible to acquire, display, and assimilate valuable sources of data into the air quality assessment process (Belsma 2004). With the launch of NASA's Terra satellite system, a part of Earth Observing System (EOS), in December 1999, satellite observation of atmospheric parameters are easier to acquire.

In most of the previous investigations of Atmospheric Smog modeling, satellite images are used to extract air pollution by calculating optical thickness in, either visible spectral ranges or low spectral resolution short-wave infra red (SWIR) and thermal infra red (TIR) ranges (RETALIS, 1999) and (Schafer et. al , 2002). Ramanathan and Ramanna (2003) tried to model aerosols in tropical regions of Asia, by low spatial resolution and high spectral resolution, NASA's Moderate Resolution Imaging Spectro-radiometer (MODIS) instrument. Their main concern was the impact of aerosols in regional radiative forcing, and precipitation. Sifakis and Soulakellis, tried to find optical thickness in VNIR and near-IR bands, in order to monitor haze with low spatial and spectral resolution MODIS data by the 'blurring effect due to scattering and backscattering induced by the aerosols. Ung et al. (Unget.al.) tried to investigate the strength of linear relationship between satellite-made observations and air quality parameters using Landsat low spatial and spectral resolution with very fewsatellite bands. They did not use any image processing software to process images.

1.4 Objective

For satellite systems with high spatial and spectral resolution and sophisticated hardware and software, it is now possible to accurately measure the level of air pollution by using TIR and SWIR bands. The objective of this research is to create a geo-spatial model based on probability density of common atmospheric pollutants in the troposphere by using feature extraction and pattern recognition technique with high-spectral and spatial resolution Earth Observation System (EOS) satellite imaging sensor Advanced Spaceborne Thermal Emission and Reflection Radiometer (ASTER) data, US Environmental Protection Agency (EPA) ground sensor data and "Analysis of Variance" of satellite pixel value with EPA ground sensor observations.

2. EXPERIMENTAL INVESTIGATION

2.1 Study Area

This research investigated three locations:

1. San Francisco Bay area, in California has a unique land feature having maritime climate surrounded by coastal ranges. In 2000 the Bay area recorded CO and PM_{10} concentration, exceeded federal standards, by 110% and 117% respectively (EPA Air Resources Board, 2005). California Air Resource Board also reported prolonged high PM_{10} emission, particularly, at Berkeley in the San Francisco Bay Area (Pacific Steel Casting Company, 2005).
2. Los Angeles, in California (a maritime climate). In Los Angeles County, Lynwood and Burbank's PM_{10} concentration recorded in the year 2003, exceeded Federal standard for 30 days (EPA Air Resources Board, 2005).

3. Charleston in mountain state of West Virginia (a humid continental climate in the Kanawha Valley). Charleston is

ranked as the sixteenth most polluted city (PM_{10} species) in USA by the American Lungs Association, year 2005 report.

2.2 Data

2.2.1 Satellite Data: ASTER is an imaging instrument flying on Terra satellite which was launched in December 1999 as part of NASA's Earth Observing System (EOS).. There are three visible and near infra-red (VNIR) bands has 15 m spatial resolution in 0.52 μ m – 0.86 μ m range, six SWIR bands has 30 m spatial resolutions in1.6 μ m – 2.43 μ m range, and five TIR bands has 90 m spatial resolution in 8.125 μ m-11.65 μ m range (2: ASTER, NASA, 2000). For this research ASTER level-1 (L1B) images. San Francisco (March 10 2000), Los Angeles (October 17, 2003) and Charleston (September 19, 2005) were chosen during fairly dry seasons and cloud free condition in order to accurately assess the atmospheric smog.

2.2.2 GIS Data: Georegistered DOQQ's of California and West Virginia sites are provided by California Spatial Information Library, Sacramento, CA, and West Virginia GIS Technological Center, Morgantown, West Virginia.

2.2.3 Air Quality Data: Air Quality Monitoring data and facilities emission data has been acquired from the United States Environmental Protection Agency (US-EPA) regional centers. The EPA data consists mainly of NO_x, CO, SO_2, PM namely, PM_{10} and $PM_{2.5}$. For this research US EPA data were taken on the same day, as that of the satellite sensor data acquisition.

Currently EPA monitoring stations use particle mass analysis instruments namely, Tapered Element Oscillating Microbalance (TEOM), Continuous Ambient Mass Monitor (CAMM), or Beta Attenuation Method Sampler (BAMS), (EPA and Air resources Board, 2005).

2.2.4 Climatic Data: Wind speed, wind direction, precipitation, humidity data of San Francisco Bay area, Los Angeles area, and Charleston are also collected from National Oceanic and Atmospheric Administration (NOAA) - National Climatic Data Center.

3. DATA PROCESSING

ASTER L1B data, of the respective sites, has been geometrically corrected and geo-registered in Universal Transverse Mercator (UTM) coordinate system, and WGS84 datum, by image-to-image registration process with DOQQ in ER-Mapper 7.1 software. Principal Component Analysis (PCA), Density Slicing (DS) and Band Ratioing (BR), technique is applied to enhance atmospheric pollutants in the imagery to model atmospheric smog in ER-mapper 7.1 software.

3.1 PCA

The PCA technique involves a mathematical procedure which transforms a number of (possibly) correlated variables into a (smaller) number of uncorrelated variables called principal components (PC). PC axes and bands of ASTER can be presented in a covariance matrix with highest variability in the image data loaded in the first PC axis and the least in the last PC axis (Jensen, 2003). PCA algorithm function uses each image band as a variable and rotates the multivariable axes about the statistical grand mean from the image dataset to transform the data axes to maximize the variability in the first PC (PC1) with the each successive component of the variability, such as second PC (PC2) and so on, loaded into each successive axis orthogonal to the previous axis. The first principal component accounts for as much of the variability in the data as possible, and each succeeding component accounts for as much of the remaining variability as possible. This maximizes the supportability of the feature and enhances the features for extraction and pattern recognition in the image. In order to extract features in the image data set PCA technique has been applied in 1-14 bands of the resultant images.

3.2 Density slicing (DS)

The DS is a form of selective one-dimensional classification. The continuous pseudocolor scale of the resultant image is "sliced" into a series of classifications based on ranges of brightness values. All pixels within a "slice" are considered to be the same information class. (Jensen, 2005). Density slicing. technique has been applied on the resultant dataset in, band 14 for HNO_3 absorption band at 11 μ m, band 7 for Carbon monoxide and carbonate absorption band at 2.3 μ m.

3.3 Band Ratioing (BR)

The BR is a process by which brightness values of satellite image pixels in one band are divided by the brightness values of their corresponding pixels in an another band in order to create an enhanced new output image. This technique is useful when there are subtle differences in signature of features in the dataset (Jensen, 2005). In this investigation band ratioing technique was found necessary only in Charleston area where all other image processing techniques were unable to distinguish cloud properties, and atmospheric pollution signatures.

4. RESULTS AND DISCUSSION

GIS map of EPA monitoring stations (Figure 1a1, 1b1, 1c1) in all areas under investigation, shows limited opportunity to assess air pollutant from in-situ data provided by EPA.

PCA image with all bands of San Francisco (Figure 1a2) and PCA image of San Francisco with VNIR and SWIR bands (Figure 1a3) shows, cloud pattern in different tones of blue and pink respectively. The different tones of colors might be mixing of various air pollutants with cloud condensation nuclei (CCN). Similarly in Los Angeles PCA image with all VNIR, SWIR and TIR bands (Figure 1b2) shows cloud pattern in different tones of blue, but the PCA image with all bands in VNIR and SWIR doesn't show any cloud pattern in different tones. This might be due to other kinds of air pollutant in the cloud mixture than that of San Francisco. In Charleston both PCA image with all VNIR, SWIR and TIR image (Figure 1c2) and with VNIR and SWIR shows different tones in blue. This might be due to mixture of different air pollutants.

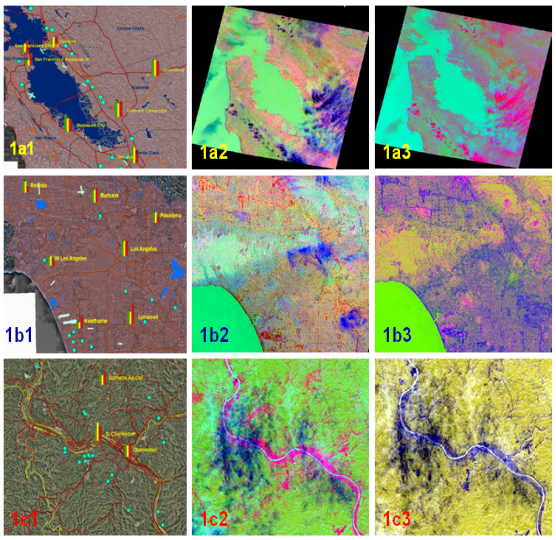

Figure 1: GIS map of industrial locations and EPA Air quality Monitoring Pollutant concentrations measured at the same time on the day of satellite data in (a1) San Francisco, (b1) Los Angeles and (c1) Charleston. Concentrations of CO are shown in green, NOx in yellow, PM_{10} in red bar graphs. (2) PCA ASTER processed images in all bands in VNIR, SWIR and TIR: (a2) San Francisco, (b2) Los Angeles and (c2) Charleston. (3) PCA ASTER processed images(RGB-PC123) in all bands in VNIR and SWIR: (a3) San Francisco, (b3) Los Angeles and (c3) Charleston.

DS image is created in pseudo color in band 14 (HNO_3 and PM_{10} absorption band), and in band 7 (carbonates absorption band). The San Francisco DS image in band 14 (Figure 2a1) and in band 7 (Figure 2a2) shows cloud pattern in different tones in brown and blue respectively clearly. But the Los Angeles DS images in band 14 (Figure 2b1) shows cloud pattern in different tone in blue and in band 7 (Figure 2b2) the cloud pattern was absent. This suggest that the cloud over Los Angeles on March 10, 2000 should have contaminats in the ASTER band 7 in frequency range 2.185 -2.225. DS image of Charleston in band 14 (Figure 2c1) and in band 7 (Figure 2c2) shows different types of cloud pattern in different tones of brown. This might be due to different kinds of pollutants that have absorption frequency in ASTER TIR band 14 (10.25-10.95) and SWIR band 7 (2.185 -2.225).

Spectral signature in graphical form is created over a cloud pattern from all ASTER imagery under investigation in all TIR and all SWIR bands seperately, by traverse technique in ER Mapper 7.1 software. In San Francisco bay area the spectral signatures of cloud pattern over a steel casting company in Berkeley, shows that SWIR band 7 and band 9 signatures are different than other SWIR bands (Figure 2a3), and that in TIR band 11 was different that all other TIR bands (Figure 2a4). In Los Angeles ASTER image the spectral signatures of cloud pattern over Commerce area shows that SWIR band 7 signature is different than all other SWIR bands (Figure 2b3), and that in all TIR bands signatures are similar (Figure 2b4). In Charleston ASTER image the spectral signatures of cloud pattern over an EPA monitoring site shows that SWIR band 5 signature is different than all other SWIR bands (Figure 2c3), but that in TIR bands 10 and14 signatures are slightly different than all other TIR bands (Figure 2c4). These signature might be coming from mixture of air column above ground and different city shows different signatures.

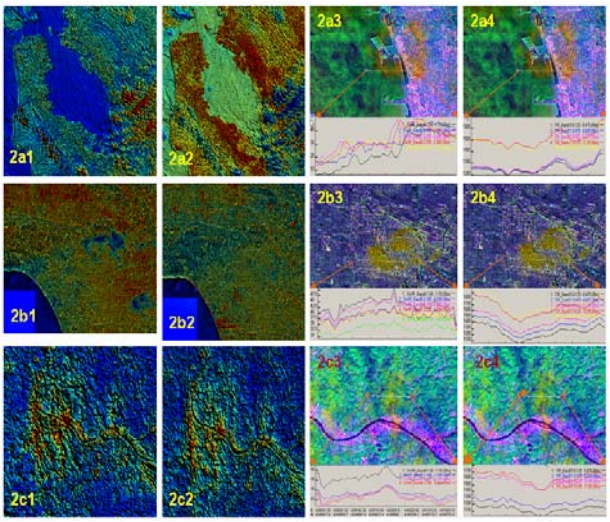

Figure2: Density sliced ASTER images (1) in band 14 and (2) band 7: (a1 and a2) San Francisco Bay area, (b1 and b2) Los Angeles, (c1 and2) Charleston. Spectral signatures compared in (3) SWIR bands (4) TIR bands: (a3 and a4) Berkeley, in San Francisco Bay area, (b3 and b4) Los Angeles, (c3 and c4) Charleston.

In view of observed slight differences in spectral signatures in particularly in bands 5, 7, 10 and 14, a band ratio image composite is created of the ASTER images with red band ratioed as 14/10 , green band ratioed as 3/5 and blue band ratioed as 3/2. The band ratio image of San Francisco (Figure3a1) shows cloud patterns in different tones colors in red and brown. The band ratio image of Los Angeles (Figure3b1) doesn't show any distinguishable cloud pattern. Where as that of Charleston shows different tones of colors in yellow. These colors might be coming from mixture of different composition in cloud properties, and different city might have different cloud composition.

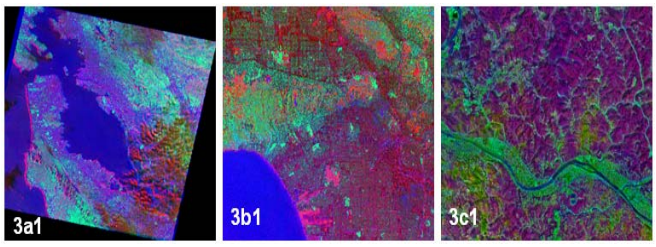

Figure3: (1) Band ratio composite image in RGB bands 3/2, 7/5, 14/10: (a1) San Francisco Bay (b1) Los Angeles area (c1) Charleston. Band pass filtering ASTER digital numbers in band 14, 7, and 3 – (2) Without High band-pass filter, (3) With High pass band filter, with: (a2 and a3) San Francisco. (b2 and b3) Los Angeles, (c2 and c31) Charleston.

5. STATISTICAL ANALYSIS

Analysis of Variance : *Analysis of variance*, or ANOVA, typically refers to partitioning the variation in a variable's values into variation among and within several groups or classes of observations. ANOVA is used to uncover the main and interaction effects of categorical independent variables (called "factors") on an interval dependent variable.

ASTER pixel values in SWIR and TIR bands, of the EPA monitoring stations of each city are used as a dependant variable and EPA measurements of pollutants as independent variables.There are different number of EPA monitoring station's air quality data in each cities, seven in Los Angeles, seven in San Francisco, and three in Charleston. Therefore there is unequal number of sample members per city; hence it is an unbalanced design. Therefore statistical procedure, 'Analysis of Variance' (ANOVA) by a 'general linear model' called 'PROC GLM' (general linear model) in SAS software (www.sas.com) is used in this investigation.

A linear model has been used in order to fit EPA in-situ data into ASTER pixel digital numbers data, (DNs) that include each city, San Francisco, Los Angeles and Charleston as a blocking factor and only they are removed from the model where they are non-significant. The linear model relationship created is as follows:

(ASTER DNs) = A +B* (EPA Pollutant Concentration) + C * (City effect)

Where A = Intercept
B= Slope
C= Regional shift

All pixel values and pollutants concentrations levels are fed into PROC-GLM program in 'SAS' software (www.sas.com). The interactions (Pollutant * City effect) were tested, with all SWIR and TIR bands, with observed significance levels (p-value 0.005) in order to determine if the data meets an acceptance level of error.

The statistical term 'Coefficient of Determination (R-Square) is a statistical term, which signifies total percentage of variations explained by the independent variable in the regression line, and rest of the variations is explained by another factor (not a linear relationship).

Results from PROC GLM program in SAS software obtained are shown in the Table-2. The lower the p-values, the more likely the effect is significant. Values were removed from these models where they were not significant. All of the assumptions were tested for all models, and only channel 9 data had to be log-transformed in order to meet the assumptions of the ANOVA. The significant City effects indicate that results are not consistent between cities (all channels for PM_10, all except Ch10 for CO, channels 10-14 for NOx). If the city effect is non-significant, the spectral response to the pollutant is consistent (Ch10 for CO and bands 10-14 for NOx). In SWIR bands ASTER bands 5 through 9 (Table2) shows no correlation with PM_10 concentrations, and only ASTER band 7 was found weakly correlated with CO concentrations. All 5 SWIR ASTER bands indicate correlations with NOx levels. In TIR bands, ASTER bands 10-14, the relationship between spectral values and CO or NO_X concentration were highly significant. Amazingly PM10 showed only week relationship with all ASTER TIR bands. This might be due to the fact that the sensitivity of satellite observation with TIR bands to atmospheric composition is small in lower mixed layer of atmosphere.

Air Pollutants		ASTER Bands									
		Short-wave Infrared Bands					Thermal Infrared Bands				
		B-5	B-6	B-7	B-8	B-9	B-10	B-11	B-12	B-13	B-14
CO	*p-values*	-	-	0.0162	-	-	0.0004	0.0003	0.0005	0.0005	0.0003
	City Effect	0.0039	0.0036	0.0007	0.0094	0.0131	-	0.0177	0.0019	0.0013	0.0001
	R-Square	0.57803	0.57972	0.69101	0.52166	0.48791	0.68999	0.72365	0.75932	0.76195	0.81558
NOx	*p-values*	0.009	0.0044	0.0007	0.0041	0.0032	0.0001	0.0001	0.0001	0.0001	0.0001
	City Effect	-	-	-	-	-	0.0015	0.0024	0.0007	0.0002	0.0001
	R-Square	0.56603	0.62248	0.67411	0.17875	0.56584	0.75379	0.77286	0.81721	0.86425	0.88177
PM_10	*p-values*	-	-	-	-	-	0.0164	0.0193	0.0466	0.0332	0.0236
	City Effect	0.0133	0.0057	0.0098	0.0293	0.0233	0.0296	0.0147	0.0071	0.0044	0.001
	R-Square	0.50157	0.54904	0.51235	0.42463	0.44043	0.46732	0.50151	0.29548	0.5695	0.65291

Table-2: Probability error level of in ASTER reflectance value in correspond to the EPA pollutants monitoring of CO, NOx and PM_10 in all cities under investigation (from 'ANOVA' ProcGLM, Program in SAS software. This table contains p-values; The (–) represents non-significant p-value (i.e.if p>0.05. Non-significant -value type of data has no statistically significant effect on overall mean.

The Coefficient of Determination (R-Square's) in SWIR channel 7 In channel 7, for CO, NOx, and PM_10 were 0.691, 0.67 and 0.54 respectively. In Channel 14, R-Square found for CO, NOx, and PM_10 were 0.815, 0.88 and 0.653, showing high sensitivity of band 14 for CO and NOx, but there is no absoption bands known for those gases, only PM10 has absorption bands in those frequencies. This may be due to mixture of gases present there and lower sensitivity of TIR satellite observations, although there is a strong absorption band for HNO3 at 11 μ in ASTER band 14. It may be also due to the fact that there were fewer number of EPA monitoring stations in this research. The possible wind factor may also causes transport of pollutant over longer distances may provide for photochemical mix and dilution of samples.

Scatter Plot of Variance: Scatter plots of Pollutant concentration with ASTER pixel digital data numbers are created for, CO, NOx and PM_10 of in bands 7 and 14, where high correlations were observed. Result shown in the scatter plots (Figure4) suggest city wise regional shifts in correlation of data swarm.

6. CONCLUSION

This research investigation presents a methodology to assess atmospheric pollution from a multi-spectral satellite platform. The GIS map cities with EPA monitoring sites suggests that there are multiple sources of air pollutants. Several image processing techniques were used to model atmospheric features. In the research investigation highlighted differences in pollution absorption patterns with the relatively wide wavelength bands of ASTER. PCA, density slicing. Band ratioing and spectral signatures in different bands demonstrated many different kinds of pollutant patterns in different cities under investigation. More accurate and detailed information on air pollutants

patterns can be assessed using hyperspectral data.. The statistical analysis supported different feature extraction patterns of different air pollutants in the atmosphere of San Francisco, Los Angeles and Charleston. More accurate and detailed information on air pollutants patterns can be assessed using hyperspectral data. Future research investigations will focus on hyperspectral studies in order to find the subtle differences in spectral signature of atmospheric constituents and pollutants.

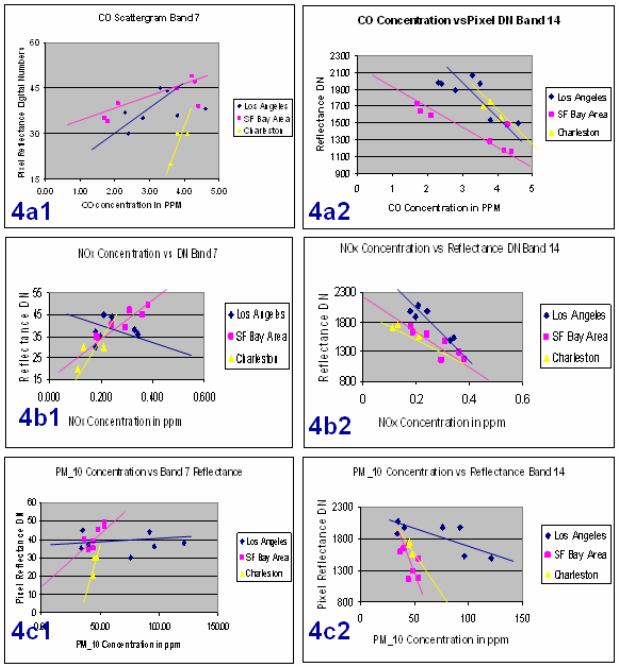

Figure 4: Scatter plot of EPA pollutant Concentration level at San Francisco Bay area, Los Angeles area, and at Charleston area against respective sites ASTER digital numbers in bands 14 and 7: (a1) and (a2) CO in band 7 and 14 respectively. (b1) and (b2) NOx in bands 7 and 14 respectively. (c1) and (c2) PM_10 in bands 7 and 14 respectively.

REFERENCES

ANOVA Tutorial: See http://www.ats.ucla.edu/STAT/sas/library/repeated_ut.htm

ASTER, NASA, 2000: ASTER user guide, NASA, 2000.

Belsma Leslie O., 'Satellite Data for Air Quality Forcaster', The Aerospace Report. 2004

Chung C. E. and V. Ramanathan, South Asian Haze Forcing: Remote Impact with Implications to ENSO and AO, American Meterological Society, June 2003, p-1791-1806

EPA: Criteria Pollutant report http://www.epa.gov/airtrends/aqtrnd98/chapter2.pdf, 1998.

EPA Air Resources Board: State and Local Monitoring Network Report manual, October 2005.

HITRAN : High-resolution Transmission Molecular Absorption database, see www.hitran.com Jensen, J. R.: Introductory Digital Image Processing: A Remote

USGS-Landsat, 1998: See the http://landsat7.usgs.gov/ Menon Surabi, James Hansen, Larissa Nazarenko, and Yunfeng Luo: Climate effects of Black Carbon Aerosols in China and India, Sciencemag.org, Vol-297, September 27, 2002.

Pacific Steel Casting Company, Berkeley, CA 94710, Summary of Pacific Steel Casting's proposed odor control plan, http://www.pacificsteel.com/OdorControlPlanSummary&Plan%202005.pdf. 2005.

Ramanathan, V. Satheesh, S.K. Large Differences in Tropical Aerosol Forcing at the Top of the Atmosphere and Earth's Surface, Nature, 405, 60, 2001.

Ramanathan, V. and M.V. Ramanna: Atmospheric Brown Clouds: Long-Range Transport and Climate Impacts, EM December 2003.

RETALIS, A: Assessment of the distribution of aerosols in the area of Athens with the use of Landsat Thematic Mapper data: International Journal of Remote Sensing, p-939 – 945. Taylor & Francis Volume 20, Number 5 / March 20, 1999.

Sifakis N. I., N.A. Soulakellis, in 'Satellite Image Processing for Haze and Aerosol Mapping (SIPHA): Code Description and presentation of results, Institute of Space Application & Remote Sensing, National Observatory of Athens: European Commission funded research, Contract number 94/.GR/A32/GR/01616/ATT. See http://www.space.noa.gr

Schafer, K. G.Fömmel[1], H.Hoffmann, S.Briz, W.Junkermann, S. Emeis,C.Jahn,S.Leipold,A.Sedlmaier,S.Dinev,G.Reishofer, L.Windholz, N.Soulakellis, N.Sifakis and D.Sarigiannis. Three-Dimensional Ground-Based Measurements of Urban Air Quality to Evaluate Satellite Derived Interpretations for Urban Air Pollution: Springer, Vol. 2, Number 5-6, September 2002.

UNEP:Atmospheric Brown Clouds, 2005 under the sponsorship of the United Nations Environmental Program and NOAA. See http://www.sianbrowncloud.ucsd.edu/.

UNEP Assessment Report, 2004: See the website: http://www.rrcap.unep.org/abc/impactstudy/Part%20I.pdf.

Ung Anthony, Lucien Wald, Thierry Ranchin, Joseph Kleinpeter: Air pollution mapping: Relationship between satellite-made observations and air quality parameters, 12th International Symposium, Transport and Air Pollution, 16-18 June 2003, p-105-111.

WHO,2000,Guidelines for Air Quality, World Health Organization Report, Geneva, 2000.

Yu H. Y.J. Kaufman, M. Chin, G. Feingold, M. Zhou A Review of Measurement-based Assessment of Aerosol Direct Radiative Effect and Forcing, Atmospheric Chemistry and Physics, May 2005.